Physics Letters B 816 (2021) 136251

Contents lists available at ScienceDirect

Physics Letters B

www.elsevier.com/locate/physletb

Jet quenching test of the QCD matter created at RHIC and the LHC needs opacity-resummed medium induced radiation

Xabier Feal *, Carlos A. Salgado, Ricardo A. Vazquez

Instituto Galego de Física de Altas Enerxías IGFAE, Universidade de Santiago de Compostela, Galicia-Spain

ARTICLE INFO

Article history:
Received 14 May 2020
Received in revised form 3 March 2021
Accepted 23 March 2021
Available online 26 March 2021
Editor: J.-P. Blaizot

ABSTRACT

After almost two decades of investigation, jet quenching has become a fundamental tool to study the properties of the QCD matter produced in high-energy nuclear collisions. Despite the large progress in both experimental and theoretical tools, several unknowns remain to be solved. In particular the systematics of the QCD matter parameters extracted at different energies and centralities is still puzzling. On the other hand, a lot of attention has been put in the last few years to a correct resummation of the multiple scatterings that the particles of the jet suffer when traversing the QCD matter. Present formalisms have substantially improved the multiple-soft or single hard scattering approximations, common in the last twenty years. We show here that medium parameters extracted with full resummed medium-induced gluon radiation spectra significantly differ from these two extreme approximations, providing natural systematics for different collision energies and centralities, with no inconsistencies. For the case of the full resummation this ensures that the density of scattering centers as a function of the temperature qualitatively agrees with the equation of state computed in lattice QCD.

The hottest matter ever created in laboratory, the quark gluon plasma (QGP), is produced by smashing large atomic nuclei in particle colliders. The QGP is thought to be the primordial material that filled the whole universe some micro-seconds after the Big Bang and measuring its properties is the main goal of the experimental programs of nuclear collisions at RHIC and LHC. These *heavy ion* programs have delivered an outstanding body of experimental evidence and novel theoretical developments supporting our current view on the QGP as a nearly inviscid, rapidly thermalized liquid, color screened to melt any hadronic bound state. Determining the properties of this phase of the matter has constituted one of the most important open problems in high energy physics and a milestone in our understanding of the theory of the strong interactions [1–3].

One of the main experimental tools in these studies is jet quenching: fast particles retain characteristic imprints of their passage through the QGP that can be measured as modifications in the high transverse momentum spectrum of the collision. A good theoretical control on the underlying dynamics is a prerequisite to relate these measured imprints with the properties of the QGP. At high enough energy, the dynamics is dominated by induced radiation of gluons. In simple quantum-mechanical terms, this radiation can be understood as the decoherence of a gluon fluctuation from the fast particle due to color-rotating multiple elastic collisions with the medium. The elementary cross section of these elastic collisions has been computed in perturbative QCD. The medium-induced gluon radiation spectrum has also been known for some time in the soft limit [4–7] and beyond the soft approximation [8,9]; see also [10,11]. In all cases, expressions for an arbitrary number of scattering centers are known — the *opacity expansion* series — but difficult to treat numerically. For this reason, two limiting cases are usually employed: i) keeping only the first term in the expansion but the full perturbative cross section (also known as $N = 1$ or single hard approximation in the following, sometimes also referred as GLV approximation); ii) resumming all multiple scatterings in Gaussian approximation, that neglects the perturbative power-law Coulomb tails (also known as BDMPS or multiple soft scattering approximation). While these two approximations have provided a good description of the suppression for a given colliding energy and centrality, a common understanding of RHIC and LHC data at different centralities and energies has been puzzling our community for almost 10 years. An inconsistent deviation by a factor $K \simeq 1.3 - 2$ in the extracted QGP opacity has been systematically found in all the phenomenological analyses to date when going from LHC to RHIC energies. Triggered by this unsatisfactory understanding of more and more precise data on jet quenching, the relevance of the resummation schemes have

* Corresponding author.
E-mail addresses: xabier.feal@igfae.usc.es (X. Feal), carlos.salgado@usc.es (C.A. Salgado), vazquez@igfae.usc.es (R.A. Vazquez).

https://doi.org/10.1016/j.physletb.2021.136251

recently received a renewed attention (see e.g. [15–18]). To this extent, it is natural to wonder whether the absence of a correct resummation may have been reabsorbed in the extracted opacity parameter as a systematic deviation. The main goal of this letter is to show that this is indeed the case, i.e. that a full resummation of scattering centers including the expected perturbative tails, modifies the systematics of the extracted medium parameters with collision energy and centrality, providing a natural solution to the above-mentioned puzzle. We find that the extracted number density (the fitting parameter in our approach) qualitatively agrees with the QGP equation of state computed in lattice QCD, while it qualitatively disagrees if the resummation is not performed. In most phenomenological studies, the QCD equation of state is an input of the calculation and the disagreement is absorbed in modified medium parameters —often through the strong coupling constant α_s. Our different strategy makes the origin of the disagreements evident, shows that the full resummation is needed for a precise determination of the medium parameters and provides a framework to determine the QGP color opacity with jet observables with no inconsistencies.

In this exploratory study, we shall not attempt to model the precise medium dynamics but adopt a simpler approach in which once the temperature at some initial time is fixed, all other quantities in the calculation, except the number density, are computed from known perturbative relations. The number density is then the free parameter in the fit of the inclusive particle suppression R_{AA} for each collision energy and centrality. Using this procedure, somehow orthogonal to the usual implementation in which the density is directly taken from e.g. hydrodynamical profiles, we can check the temperature dependence of the number density and perform the qualitative comparisons[1] with available results from lattice QCD on the equation of state that we have mentioned above.

To evaluate the gluon bremsstrahlung we will follow [19] and discretize the gluon path in n steps of length $\delta z = 0.1\lambda_g$, where λ_g is the gluon mean free path. The gluon four momenta is given by $k^l = (\omega, \boldsymbol{k}^l)$ for $l = 1, \ldots, n$. Soft gluons in this picture can be emitted from any of the l-th internal lines or from the last n-th leg. These two classes of diagrams can be accounted for with color-factorized 4-currents J^l and J^n, respectively, whose components in the Coulomb gauge read

$$J^l_i = \epsilon_{ijk}\frac{k^l_j p_k}{k^l_\mu p^\mu}\left(e^{i\varphi^n_{l+1}} - e^{i\varphi^n_l}\right), \quad J^n_i = \epsilon_{ijk}\frac{k^n_j p_k}{k^n_\mu p^\mu}, \tag{1}$$

and $J^l_0 = J^n_0 = 0$. Here, the hard particle 4-momentum p has been left fixed along the initial direction and ϵ_{ijk} is the Levi-Civita symbol. The decoherence of phases φ^a_b between gluon interactions at a and b modulates the non-Abelian LPM suppression [20–22], and reads

$$\varphi^n_l = \frac{1}{p_0}\sum_{i=l}^{n-1}\delta z_i k^i_\mu p^\mu, \quad \delta z_i = z_{i+1} - z_i, \tag{2}$$

where z_i is the path discretization along the traveling direction and p_0 the hard particle energy. The total intensity is measured with respect to the (zeroth order) radiation at the hard production vertex [5,23], i.e. the radiation still present in the absence of a medium,

$$J^2_T(k) = \left|J^n + \sum_{l=1}^{n-1} J^l\right|^2 - \left|J^n\right|^2, \tag{3}$$

and has to be evaluated within the internal gluon momentum distributions. In a tagged parton scenario in which color and spatial averages can be taken, event by event fluctuations fade out and the gluon in-medium dynamics can be stochastically built with the knowledge of the color averaged cross section of changing momentum $\boldsymbol{q}$ into a single collision, whose Fourier transform reads

$$\sigma(\boldsymbol{x}) \equiv \int \frac{d^2\boldsymbol{q}}{(2\pi)^2} e^{-i\boldsymbol{q}\cdot\boldsymbol{x}} \frac{1}{d_A d_R}\mathrm{Tr}\left(F^\dagger_{el}(\boldsymbol{q})F_{el}(\boldsymbol{q})\right), \tag{4}$$

with $d_A = N_c^2 - 1$ and $d_R = N_c$ ($d_R = N_c^2 - 1$) the color dimension of the target quark (gluon). For the relevant temperatures of the hot medium the single scattering amplitudes can be expanded at leading order in the coupling as $F_{el}(\boldsymbol{q}) = -ig_s^2 t^A_\alpha t^R_\alpha/(\boldsymbol{q}^2 + \mu_d^2)$ with $g_s^2 = 4\pi\alpha_s$, where t_A and t_R are SU(3) matrices in the gluon and the target representation and $\mu_d = 1/r_d$ the screening mass of the color field of a single scattering center. After an arbitrary number of collisions governed by (4), the probability of emerging with momentum change $\boldsymbol{q}$ in a medium path s is given by

$$\phi(q,s) = 2\pi\delta(q^0)\int d^2\boldsymbol{x}e^{i\boldsymbol{q}\cdot\boldsymbol{x}}\exp\int_0^s dz\rho(z)\Big[\sigma(\boldsymbol{x}) - \sigma(\boldsymbol{0})\Big], \tag{5}$$

where $\rho(z)$ is the local number density of the medium at a depth z. This distribution satisfies the Moliere QCD equation with kernel (4) and inherits, though with larger widths linear with l, the long $\boldsymbol{q}$ tails of the single scattering scenario. The intensity of soft gluons emitted in an in-medium path l in the energy interval ω and $\omega + d\omega$ per unit of time and per unit of medium transverse size satisfies the weighted convolution of (3) with (5)

$$\omega\frac{dI}{d\omega} = \alpha_s C_R\int\frac{d\Omega_n}{(2\pi)^2}\left(\prod_{k=0}^{n-1}\int\frac{d^3\boldsymbol{k}_k}{(2\pi)^3}\phi(q_k,\delta z_k)\right)J^2_T(k), \tag{6}$$

with Ω_n the gluon solid angle, $C_R = 4/3$ (3) the color averaged charge of the squared vertex $q \to qg$ ($g \to gg$) and $q_k = k_{k+1} - k_k$. For consistency within the soft gluon approximation the splitting function corrections [24,9] are here omitted.[2] The expression given above Eq. (6) can be interpreted in probabilistic terms and is suitable for a Monte Carlo evaluation by summing over many gluon in-medium paths of length l. In the continuous limit path integrals on the light cone are recovered [25]. In addition, evaluation of Eq. (6) in an expanding medium is straightforward. Closed results, like the GLV [6,26] and BDMPS-ASW [5,23,27–29] predictions for small and arbitrary opacities, respectively, can be obtained from Eq. (6) either with perturbative expansions or by assuming Brownian elastic scattering respectively [25]. Multiple hard interactions in semi-infinite media have been also resummed before not exactly considering the radiation scenario after the hard production vertex [30] or making use of the Gaussian approximation [24], and then later extended for the finite case [31]. Radiation (6) has a typical width characterized by the scale $\omega_c \simeq 1/2\hat{q}l^2$ [5,23,28], where $\hat{q}$ is the QGP transport coefficient. Gluons of energy $\omega > \omega_c$ are not able to resolve the medium [19] and thus radiation vanishes slowly with large tails $\propto 1/\omega$. At the smallest energies $\omega \leq \mu_d$ kinematical constraints also cancel the radiation.

Our numerical implementation of the formalism described in eqs. (1)-(6) allows to perform the exact resummation of the multiple scattering contributions with realistic scattering potentials –

[1] We work under the assumption that the QGP admits a quasiparticle interpretation for which our perturbative description would be adequate – see also [14]. For an ideal gas the number density can be directly related to other thermodynamical quantities, but this is not the case for an interacting QGP and this is why our comparison has to be taken at the qualitative level at this stage.

[2] We have checked that for the most central *PbPb* collisions ($\sqrt{s_{NN}} = 2.76$ TeV) this results in medium density underestimations of $\sim 22\%$.

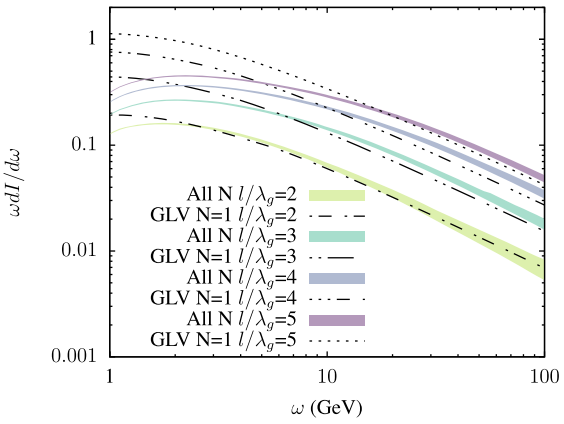

Fig. 1. Medium induced gluon radiation for a QGP brick involving $l/\lambda_g = 2, 3, 4$ collisions on average, in the N=1 term in an opacity expansion (GLV) and the full resummation.

we have used a Debye potential but very similar results can be obtained for thermal potential [17]. In Fig. 1 we present our full results compared with the case in which only a single scattering is considered for different opacity parameters of relevance for the present phenomenological study. One clearly sees that increasing the average number of scattering centers makes the spectrum to depart more and more from the single scattering case which has the tendency to overpopulate the soft gluon radiation. As a consequence, when the density of the medium grows (e.g. when going from lower to higher collision energies) overestimating the soft gluon radiation translates into an artificially larger energy loss that can only be compensated by the corresponding reduction of the medium parameters in order to reproduce the experimental data.[3] We identify this as the main effect in the energy and centrality puzzle for the systematics of the medium parameters.

We should notice that under the intensity (6) more than a single gluon is usually emitted. For soft gluon emission, when the formation time is much smaller than the length of the medium, the daughter partons in the splitting lose color coherence very fast and an independent gluon emission is justified [10,8]. Here, we take the usual Poisson approximation for the probability $P(\epsilon, p_t)$ of a hard parton of energy p_t to lose an energy ϵ —also known as the quenching weight [32,28],

$$P(\epsilon, p_t) = \mathcal{N} \sum_{n=0}^{\infty} \frac{1}{n!} \delta\left(\epsilon - \sum_{i=1}^{n} \omega_i\right) \prod_{i=1}^{n} I\left(p_t - \sum_{j=1}^{i-1} \omega_j\right), \tag{7}$$

where the average number of gluons, $I(p_t)$, and the probability of no emission $N(p_t)$, are functions of the initial energy

$$I(p_t) = \int_0^{p_t} d\omega \frac{dI}{d\omega}, \qquad N(p_t) = e^{-I(p_t)}. \tag{8}$$

In this work, we are interested in the suppression of inclusive particle production at large transverse momentum, where the detected particle is not a parton i, but a given hadron, h, carrying away a fraction z of the parton energy with probability $D_i^h(z)$. The abundance of hard events may be assumed to scale with the number of hard processes in a single nucleon-nucleon collision [33] and within these pQCD assumptions the quenched inclusive hadron cross section reads [32,34]

$$\frac{d\sigma_{AA}^h(p_t)}{dydp_t} = T_{AA} \sum_i \int dz D_i^h(z) \int_0^{\infty} d\epsilon \frac{d\sigma_{pp}^i(p_t/z + \epsilon)}{dydp_t} P_i(\epsilon, p_t/z + \epsilon), \tag{9}$$

where T_{AA} is the nuclear overlap function. In order to make the numerical computations treatable, in this first study we consider $P_i(\epsilon, p_t/z + \epsilon)$ to be smooth enough to allow an evaluation at the typical fragmentation ratio $\langle z \rangle$ to find [28,32]

$$\frac{d\sigma_{AA}^h(p_t)}{dydp_t} \simeq T_{AA} \sum_i \int_0^{\infty} d\epsilon \frac{d\sigma_{pp}^{i,h}(p_t + \epsilon)}{dydp_t} P_i(\epsilon, p_t + \epsilon), \tag{10}$$

with i running over gluons and the different quark species. This approximation has been frequently used (see e.g. [28,32,34]) as it provides a quite precise answer with a much simpler numerical implementation, as discussed also in [35]. Direct calculations of the sensitivity of the hadron spectrum suppression to different fragmentation function scenarios are also known to be small —see e.g. [36]. Hadron fragmentation, typically to pions, takes place via the gluon channels at small p_t and it is dominated by quarks starting from p_t around 30 GeV to 100 GeV for $\sqrt{s_{nn}} = 0.9$ TeV to 7 TeV, depending on the different fragmentation implementations [37,38]. Since gluons lose noticeably more energy than quarks due to their larger color space factor in (4) and (6), the suppression of high-p_t hadrons will be larger when they originate from gluons than for quarks. In order to implement this difference we take the gluon-to-quark ratio in the hadronic spectrum to be

$$\frac{d\sigma_{pp}^{g,h}(p_t)}{dydp_t} \Big/ \sum_i \frac{d\sigma_{pp}^{i,h}(p_t)}{dydp_t} = 1 - \frac{1}{2p_t^c} p_t, \tag{11}$$

with the quark/gluon turnover around $p_t^c \simeq 60$ GeV fixed for all the collision energies explored in this work. In this simplified treatment of the perturbative spectrum we just classify the parent partons in gluons or quarks, irrespectively of the flavor, so the sum in the denominator of Eq. (11) runs over all quark flavors. This setup fulfills the single gluon (quark) channel scenario at $p_t \simeq 0$ ($p_t \simeq 2p_t^c$), respectively, and deviates only a $\sim 10\%$ from some fragmentation implementations [38]. We have checked that this deviation translates into QGP density predictions affected by $\sim 8\%$ at the most central *PbPb* collisions ($\sqrt{s_{nn}}$ =2.76 TeV). As usual, the nuclear modification factor is given by

$$R_{AA}^h \equiv \frac{1}{\langle T_{AA} \rangle} \frac{d\sigma_{AA}^h(p_t)}{dydp_t} \Big/ \frac{d\sigma_{pp}^h(p_t)}{dydp_t}. \tag{12}$$

Finally, the pp inclusive hadronic cross section in (12) is taken in this analysis directly from the experimental data, so that no further uncertainty is needed.

The inputs to the spectrum (6), that completely determines the energy loss distribution (7) and, hence, the suppression (12), are the Debye screening mass μ_D, the running coupling α_s, the medium length traversed by the parton l and the density of scattering centers ρ, that is the only fitting parameter in our approach. We discuss now how we fix these different inputs.

After formation the QGP thermalizes at some temperature T_0 in a time $\tau_0 \lesssim 1$ fm/c following non-equilibrium dynamics. We will simply assume that thermalization is achieved quicker when

[3] In fact, the actual effect is a bit more complicated as it involves the different slopes in the perturbative spectrum convoluted with the energy loss probabilities. These slopes are smaller at larger energies — the spectra of produced particles is harder — making it more sensitive to the infrared.

the number of collisions is larger $\tau_0 \propto 1/T_0$ [39,40]. The system subsequently expands and cools down with lifetimes of the order $\lesssim$ 10 fm/c according to event by event dynamics that can be only accessed through precise hydrodynamical or kinetic theory calculations (see e.g. [41] for a recent review). The fast parton quenching, however, is mostly sensitive to the microscopic scales μ_d and the path-averaged macroscopic opacity in ω_c [42,43], i.e. to the average number of collisions along the path of its travel. It has become customary to obtain these local properties from hydrodynamical studies of the heavy-ion collision data in the soft part of the spectrum. Here, however, this usual prescription would prevent us to check the (qualitative) agreement of the temperature dependence of the number density with the equation of state. For this reason, we assume a simple one-dimensional longitudinal expansion [44,45] $\rho(\tau) = \rho(\tau_0)\tau_0/\tau$ and accurate estimations of the QGP lifetimes through Bose-Einstein pion correlations [46,47]. Several works have shown that the experimental accuracy of R_{AA} is not enough to distinguish between different hydrodynamical profiles — see e.g. [12].

In order to fix the length that the parton travels through matter, we consider that the typical lifetimes of the QGP are usually smaller than its initial transverse dimensions, varying in the most central collisions from $\tau_f = 7.3 \pm 0.2$ fm/c in *AuAu* collisions ($\sqrt{s_{nn}} = 200$ GeV) to around $\tau_f = 9.8 \pm 0.9$ fm/c in *PbPb* collisions ($\sqrt{s_{nn}} = 2.76$ TeV). The combined data can be parameterized into a single expression $\tau_f = (0.87 \pm 0.01) \times (dN_{ch}/d\eta)^{1/3}$ fm/c, deviating less than a 10% from the RHIC and LHC predictions with freeze-out at $T_f \simeq 120$ MeV [48,49]. We will only attempt here to evaluate (12) for the averaged in-medium path length constrained by these HBT system sizes. For typical $p_t \gtrsim 5$ GeV the interactions with the cold nuclear matter can be neglected [50], then on average the fast parton travels a distance

$$l \simeq \int_0^{\tau_f} p(s) s ds + \tau_f \int_{\tau_f}^{2R} p(s) ds, \tag{13}$$

subject to the hot medium quenching, where for simplicity and within our current uncertainties isotropic production may be assumed $p(s) = \sqrt{4R^2 - s^2}/(R^2\pi)$ and R is the radius of the nuclear overlapping area. A more precise implementation of the path fluctuations and the hard production anisotropies are required for a better treatment of the low p_t regime and the most peripheral collisions. Typical in-medium path lengths are found at the largest RHIC energies 10-20% smaller than their LHC counterparts. The effective volume found by the parton within this setup is in very good agreement, in the analyzed range of centralities, with the hydrodynamical predictions at the freeze-out [51].

The running coupling is set at leading order $\alpha_s(q) = 1/(b_0 \ln(q^2/\Lambda^2))$, with $b_0 = (33 - 2N_f)/12\pi$ the 1-loop β-function coefficient for $N_f = 2 + 1$ active flavors. The latest world average at the Z^0 mass $\alpha_s(M_Z^2) = 0.1181 \pm 0.0011$ fixes the QCD scale at $\Lambda_s = 247$ MeV [52]. This setup reproduces well the collected data below $\alpha_s(m_\tau) = 0.325 \pm 0.015$ and then it shall be considered safe for the collision energies explored in this work. The screening length of the QGP may be set with the help of the HTL [53,54] result $\mu_d^2(T) = 4\pi\alpha_s(2\pi T)(1 + N_f/6)T^2$ which within the above coupling setup and the running scale set to $q = 2\pi T$ matches the heavy-quark free energy predictions in quenched lattice computations ($N_f = 0$) and falls a 10% below the full QCD result with two flavors in the staggered quark action [55].

We have made an analysis of existing data on jet quenching, including *CuCu* and *AuAu* data at 200 GeV [56,57], *PbPb* at 2.76 TeV [58–60], *PbPb* at 5.02 TeV [61,62], and *XeXe* data at 5.44 TeV [63]. For each centrality and energy considered a fit is made to the nuclear modification factor R_{AA}^h using ρ_0 as the single unknown parameter. To determine the initial temperature of each analyzed collision system, energy and centrality we used $\epsilon\tau_0 \propto T_0^3$ measurements, when available, and extrapolated the relation $\epsilon\tau_0 \simeq (8.85 \pm 0.44) \times (\sqrt{s_{nn}})^{0.33\pm0.02}$ GeV^2/fm for the most central collisions between $\sqrt{s_{nn}} = 27$ GeV-2.76 TeV, when measurements have not yet been made available [64,65]. We then fix as a reference the most central *PbPb* collisions at $\sqrt{s_{nn}} = 2.76$ TeV to a temperature of $T_0 \simeq 470$ MeV [66] and $\tau_0 = 0.6$ fm. This temperature then fixes with a single setup all the parameters in the analysis, whose temperature dependence was explained in the last paragraphs, except ρ_0, which is taken as the free parameter for each centrality, energy and collision system.

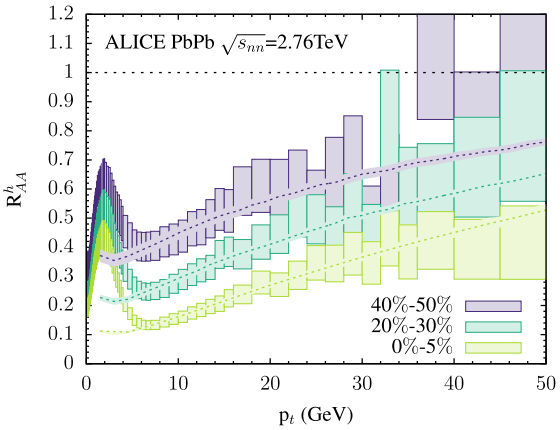

Fig. 2. Nuclear modification factor R_{AA}^h as a function of transverse energy p_t for a QGP with initial density at the most central class $\rho_0 \simeq 56/\text{fm}^3$, $\alpha_s \simeq 0.28$, $\mu_d \simeq 1.1$ GeV, $\tau_0 \simeq 0.6$ fm/c and lifetime $\tau_f \simeq 9.8$ fm/c fitted to ALICE data [59].

As a first example, fitting the most central *PbPb* collisions at $\sqrt{s_{nn}} = 2.76$ TeV yields $\rho(\tau_0) \simeq 56$ fm^{-3}. The fit for this example case is shown in Fig. 2, where we plot R_{AA}^h as a function of p_t for three centrality classes and include in the caption the numerical values of the QGP parameters obtained for the most central data. The initial density is found to scale roughly proportional to $N_{part}^{1/2} \propto T_0^3$ at fixed collision energy. At the largest RHIC energies $\sqrt{s_{nn}} = 200$ GeV in the most central *AuAu* collisions the initial temperature extracted from the energy density measurements yields $T_0 \simeq 362$ MeV and the density obtained in the fit $\rho(\tau_0) \simeq 21$ fm^{-3}.

Our results on the fitting parameter ρ scale roughly constant with T^3, in agreement with expectations. The same analysis using the single hard approximation to the gluon radiation, produces instead progressive deviations with centrality in the scale ρ/T^3. A deviation factor of $K = 1.22$ in ρ/T^3 is found between the hottest QGP created at RHIC and the most central collisions of *PbPb* at $\sqrt{s_{nn}} = 2.76$ TeV by using the single hard approximation. With the coupling and tail logarithmic corrections, this translates into a deviation of $K = 1.29$ in $\hat{q}$,

$$\hat{q} = 2\pi\alpha_s^2 C_R \rho_0 \left(\log\left(\frac{2p_0}{\mu_d}\right) - \frac{1}{2}\right) \tag{14}$$

the QGP transport parameter. This finding is consistent with the value $K \simeq 1.3$ found by previous perturbative analyses [13]. These results for $\hat{q}$ are shown in Fig. 3 and compared with the energy puzzles found by [13]. While the single hard approximation ($N = 1$) provides a reasonable estimation of the $1/\omega$ tails of the radiation for the RHIC and LHC scenarios - involving few collisions in general $n_c \lesssim 5$ -, we have checked that large uncertainties, related to the neglect of the soft resummations and the non-collinear effects, are behind these energy puzzles. Similar deviations, however with larger factors $K \simeq 2$, have been also found by the Gaussian

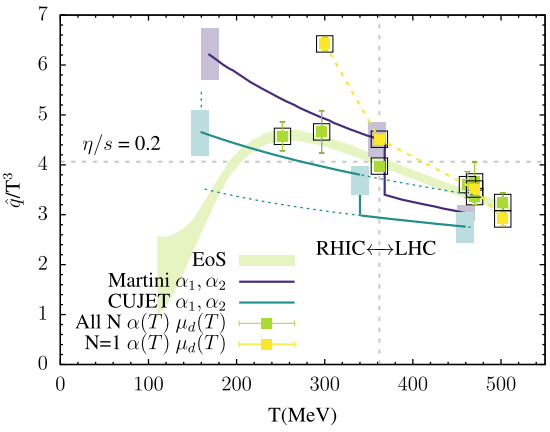

Fig. 3. QGP transport parameter $\hat{q}$ for a gluon of ω =10 GeV, using the density extracted from all order (green squares) or a first order (yellow squares) jet quenching analysis of same data as Fig. 3. Also shown in the $\hat{q}$ assuming $\rho = p/T^4$ from lattice predictions of the QCD Equation of State [67] (green band), and the CUJET (blue) and MARTINI (purple) puzzles found in [13].

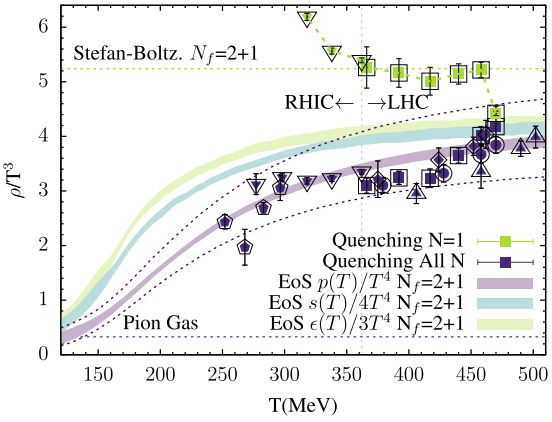

Fig. 4. QGP density extracted from All N (purple symbols) and $N = 1$ (green symbols) analyses of the R^h_{AA} collected data on collisions of *CuCu* (pentagons) and *AuAu* (down triangles) at $\sqrt{s_{nn}} = 200$ GeV, *PbPb* at $\sqrt{s_{nn}} = 2.76$ TeV (squares and circles), *PbPb* at $\sqrt{s_{nn}} = 5.02$ TeV (up triangles) and *XeXe* at $\sqrt{s_{nn}} = 5.44$ TeV (diamonds) from PHENIX, ALICE and CMS Collaborations, compared to lattice results of the Equation of State by the Wuppertal collaboration [67].

resummations of the gluon spectrum [12], where the hard tails are instead neglected. We then argue that, for a consistent description of the color opacity and $\hat{q}$ without temperature issues, an accurate implementation of the underlying quenching mechanisms is necessary beyond the single hard (GLV) and the multiple soft (BDMPS) approximations.

The ratio of the fitting parameter $\rho(\tau_0)$ with the initial temperature T_0 is plotted in Fig. 4 for all the different collision systems, energies and centralities considered. Also shown is the lattice result of p/T^4, $s/(4T^3)$, and $\epsilon/(3T^4)$ with $N_f = 2 + 1$ [67]. A global uncertainty of the 17% − 28% if fragmentation and splitting function effects were considered — is marked with bands, indicating a 10% of variation of all the unknown parameters in our study. The trend of our results agree well, without temperature issues with the rescaled QCD equation of state. For an ideal relativistic gas, it is verified that $\rho/T^3 = p/T^4 = s/(4T^3) = \epsilon/(3T^4)$, however, for an interacting quark gluon plasma, this is not the case and the agreement should be taken at the qualitative level. Our results provide then an interesting phenomenological approach to study the high temperature behavior of the color opacity of the QGP, as seen by the fast traveling partons in the collision. Collisional energy losses [68] are also neglected here and may also affect the low p_t fit. Although further studies are required, this result indicates that accurate resummations of the medium-induced gluon radiation, like the one presented in this letter, do solve the jet quenching energy puzzles between RHIC and the LHC and may open up an additional handle on the study of the QCD equation of state, for which a more rigorous connection between the jet quenching parameters and the QGP thermodynamical quantities would be needed.

Declaration of competing interest

The authors declare that they have no known competing financial interests or personal relationships that could have appeared to influence the work reported in this paper.

Acknowledgements

We thank useful discussions with Carlota Andrés, Néstor Armesto, and Pía Zurita. This work has been funded by Ministerio de Ciencia e Innovación of Spain under project FPA2017-83814-P; Unidad de Excelencia María de Maetzu under project MDM-2016-0692; ERC-2018-ADG-835105 YoctoLHC; and Xunta de Galicia (Consellería de Educación) and FEDER under Centro Singular de Investigación accreditation (2019-2022); X.F. is supported by grant ED481B-2019-040 (Xunta de Galicia) and the Fulbright Visiting Scholar fellowship.

References

[1] Y. Akiba, et al., The Hot QCD White Paper: Exploring the Phases of QCD at RHIC and the LHC, Preprint, arXiv:1502.02730.
[2] Z. Citron, et al., Future physics opportunities for high-density QCD at the LHC with heavy-ion and proton beams, CERN-LPCC-2018-07, arXiv:1812.06772.
[3] A. Dainese, et al., Heavy ions at the Future Circular Collider, CERN-TH-2016-107 arXiv:1605.01389.
[4] B.G. Zakharov, Fully quantum treatment of the Landau-Pomeranchuk-Migdal effect in QED and QCD, JETP Lett. 63 (1996) 952–957.
[5] R. Baier, Yu.L. Dokshitzer, A.H. Mueller, S. Peigne, D. Schiff, Radiative energy loss of high-energy quarks and gluons in a finite volume quark - gluon plasma, Nucl. Phys. B 483 (1997) 291.
[6] M. Gyulassy, P. Levai, I. Vitev, NonAbelian energy loss at finite opacity, Phys. Rev. Lett. 85 (2000) 5535.
[7] U.A. Wiedemann, Gluon radiation off hard quarks in a nuclear environment: Opacity expansion, Nucl. Phys. B 588 (2000) 303.
[8] L. Apolinário, N. Armesto, J.G. Milhano, C.A. Salgado, Medium-induced gluon radiation and color decoherence beyond the soft approximation, JHEP 1502 (2015) 119.
[9] M.D. Sievert, I. Vitev, Quark branching in QCD matter to any order in opacity beyond the soft gluon emission limit, Phys. Rev. D 98 (2018) 094010.
[10] J.P. Blaizot, F. Dominguez, E. Iancu, Y. Mehtar-Tani, Medium-induced gluon branching, JHEP 01 (2013) 143.
[11] B.G. Zakharov, Light cone path integral approach to the Landau-Pomeranchuk-Migdal effect, Phys. Atom. Nucl. 61 (1998) 838–854.
[12] C. Andres, N. Armesto, M. Luzum, C.A. Salgado, P. Zurita, Energy versus centrality dependence of the jet quenching parameter $\hat{q}$ at RHIC and LHC: a new puzzle?, Eur. Phys. J. C 76 (9) (2016) 475.
[13] K.M. Burke, et al., Jet Collaboration, Extracting the jet transport coefficient from jet quenching in high-energy heavy-ion collisions, Phys. Rev. C 90 (2014) 014909.
[14] F. D'Eramo, M. Lekaveckas, H. Liu, K. Rajagopal, Momentum Broadening in Weakly Coupled Quark-Gluon Plasma (with a view to finding the quasiparticles within liquid quark-gluon plasma), JHEP 1305 (2013) 031.
[15] Y. Mehtar-Tani, Gluon bremsstrahlung in finite media beyond multiple soft scattering approximation, JHEP 1907 (2019) 057.
[16] M.D. Sievert, I. Vitev, B. Yoon, A complete set of in-medium splitting functions to any order in opacity, Phys. Lett. B 795 (2019) 502.
[17] C. Andres, L. Apolinário, F. Dominguez, Medium-induced gluon radiation with full resummation of multiple scatterings for realistic parton-medium interactions, arXiv:2002.01517 [hep-ph].
[18] J. Barata, Y. Mehtar-Tani, Improved opacity expansion at NNLO for medium induced gluon radiation, arXiv:2004.02323 [hep-ph].
[19] X. Feal, R.A. Vazquez, Intensity of gluon bremsstrahlung in a finite plasma, Phys. Rev. D 98 (2018) 074029.
[20] L. Landau, I. Pomeranchuk, The limits of applicability of the theory of bremsstrahlung by electrons and of the creation of pairs at large energies, Dokl. Akad. Nauk Ser. Fiz. 92 (1953) 535.

[21] L. Landau, Electron-cascade processes at ultra-high energies, Dokl. Akad. Nauk Ser. Fiz. 92 (1953) 735.
[22] A.B. Migdal, Bremsstrahlung and Pair Production in Condensed Media at High Energies, Phys. Rev. 103 (1956) 1811.
[23] R. Baier, Yu.L. Dokshitzer, A.H. Mueller, S. Peigne, D. Schiff, Radiative energy loss and $p(T)$ broadening of high-energy partons in nuclei, Nucl. Phys. B 484 (1997) 265.
[24] B.G. Zakharov, Fully quantum treatment of the Landau-Pomeranchuk-Migdal effect in QED and QCD, JETP Lett. 63 (1996) 952.
[25] X. Feal, University of Santiago de Compostela, PhD Thesis, arXiv:1812.06903.
[26] S. Wicks, Up to and beyond ninth order in opacity: Radiative energy loss with GLV, Preprint, arXiv:0804.4704.
[27] U.A. Wiedemann, Transverse dynamics of hard partons in nuclear media and the QCD dipole, Nucl. Phys. B 582 (2000) 409.
[28] C.A. Salgado, U.A. Wiedemann, Calculating quenching weights, Phys. Rev. D 68 (2003) 014008.
[29] N. Armesto, C.A. Salgado, U.A. Wiedemann, Medium-induced gluon radiation off massive quarks fills the dead cone, Phys. Rev. D 69 (2004) 114003.
[30] P. Arnold, G.D. Moore, L.G. Yaffe, Photon and gluon emission in relativistic plasmas, JHEP 0206 (2002) 030.
[31] S. Caron-Huot, C. Gale, Phys. Rev. C 82 (2010) 064902, https://doi.org/10.1103/PhysRevC.82.064902.
[32] R. Baier, Yu.L. Dokshitzer, A.H. Mueller, D. Schiff, Quenching of hadron spectra in media, JHEP 0109 (2001) 033.
[33] M.L. Miller, K. Reygers, S.J. Sanders, P. Steinberg, Glauber modeling in high energy nuclear collisions, Ann. Rev. Nucl. Part. Sci. 57 (2007) 205.
[34] F. Arleo, Quenching of Hadron Spectra in Heavy Ion Collisions at the LHC, Phys. Rev. Lett 119 (2017) 062302.
[35] K.J. Eskola, H. Honkanen, C.A. Salgado, U.A. Wiedemann, The Fragility of high-p(T) hadron spectra as a hard probe, Nucl. Phys. A 747 (2005) 511–529.
[36] C. Andres, N. Armesto, H. Niemi, R. Paatelainen, C.A. Salgado, Jet quenching as a probe of the initial stages in heavy-ion collisions, Phys. Lett. B 803 (2020) 135318.
[37] R. Sassot, P. Zurita, M. Stratmann, Inclusive Hadron Production in the CERN-LHC Era, Phys. Rev. D 82 (2010) 074011.
[38] D. d'Enterria, K.J. Eskola, I. Helenius, H. Paukkunen, Confronting current NLO parton fragmentation functions with inclusive charged-particle spectra at hadron colliders, Nucl. Phys. B 883 (2014) 615.
[39] G. Baym, Thermal equilibration in ultra-relativistic heavy-ion collisions, Phys. Lett. B 138 (1984) 18.
[40] R. Baier, P. Romatschke, D.T. Son, A.O. Starinets, M.A. Stephanov, Relativistic viscous hydrodynamics, conformal invariance, and holography, JHEP 0804 (2008) 100.
[41] M. Strickland, Small system studies: A theory overview, Nucl. Phys. A 982 (2019) 92.
[42] C.A. Salgado, U.A. Wiedemann, Dynamical Scaling Law for Jet Tomography, Phys. Rev. Lett. 89 (2002) 092303.
[43] M. Djordjevic, U.W. Heinz, Radiative Energy Loss in a Finite Dynamical QCD, Medium Phys. Rev. Lett. 101 (2008) 022302.
[44] J.D. Bjorken, Highly relativistic nucleus-nucleus collisions: The central rapidity region, Phys. Rev. D 27 (1983) 140.
[45] R. Baier, Yu.L. Dokshitzer, A.H. Mueller, D. Schiff, Radiative energy loss of high energy partons traversing an expanding QCD plasma, Phys. Rev. C 58 (1998) 1706.
[46] A.N. Makhlin, Yu.M. Sinyukov, Hydrodynamics of Hadron Matter Under Pion Interferometric Microscope, Z. Phys. C 39 (1988) 69.
[47] F. Retiere, M.A. Lisa, Observable implications of geometrical and dynamical aspects of freeze-out in heavy ion collisions, Phys. Rev. C 70 (2004) 044907.
[48] J. Adams, et al., STAR Collaboration, Pion interferometry in Au+Au collisions at $\sqrt{s_{NN}} = 200$ GeV, Phys. Rev. C 71 (2005) 044906.
[49] J. Adam, et al., ALICE Collaboration, Centrality dependence of pion freeze-out radii in Pb-Pb collisions at $\sqrt{s_{NN}} = 2.76$ TeV, Phys. Rev. C 93 (2015) 024905.
[50] S. Acharya, et al., ALICE Collaboration, Transverse momentum spectra and nuclear modification factors of charged particles in pp, p-Pb and Pb-Pb collisions at the LHC, JHEP 1811 (2018) 013.
[51] F.G. Gardim, G. Giacalone, M. Luzum, J.-Y. Ollitrault, Revealing QCD thermodynamics in ultrarelativistic nuclear collisions, Preprint, arXiv:1908.09728.
[52] M. Tanabashi, et al., Particle Data Group, Review of Particle Physics, Phys. Rev. D 98 (2018) 030001.
[53] E. Braaten, R.D. Pisarski, Soft Amplitudes in Hot Gauge Theories: A General Analysis, Nucl. Phys. B 337 (1990) 569.
[54] A.K. Rebhan, The NonAbelian Debye mass at next-to-leading order, Phys. Rev. D 48 (1993) R3967.
[55] O. Kaczmarek, F. Zantow, Static quark-antiquark interactions in zero and finite temperature QCD: I. Heavy quark free energies, running coupling, and quarkonium binding, Phys. Rev. D 71 (2005) 114510.
[56] A. Adare, et al., PHENIX Collaboration, Onset of π^0 Suppression Studied in Cu+Cu Collisions at $\sqrt{s_{nn}} = 22.4$, 62.4, and 200 GeV, Phys. Rev. Lett. 101 (2008) 162301.
[57] A. Adare, et al., PHENIX Collaboration, Suppression pattern of neutral pions at high transverse momentum in Au + Au collisions at $\sqrt{s_{nn}} = 200$ GeV and constraints on medium transport coefficients, Phys. Rev. Lett. 101 (2008) 232301.
[58] S. Chatrchyan, et al., CMS Collaboration, Study of high-p T charged particle suppression in PbPb compared to pp collisions at $\sqrt{s_{NN}} = 2.76$ TeV, Eur. Phys. J. C 72 (2012) 1945.
[59] B. Abelev, et al., ALICE Collaboration, Centrality dependence of charged particle production at large transverse momentum in Pb-Pb collisions at $\sqrt{s_{NN}} = 2.76$, TeV Phys. Lett. B 720 (2013) 52.
[60] K. Aamodt, et al., ALICE Collaboration, Centrality dependence of the charged-particle multiplicity density at midrapidity in Pb-Pb collisions at $\sqrt{s_{NN}} = 2.76$ TeV, Phys. Rev. Lett. 106 (2011) 032301.
[61] V. Khachatryan, et al., CMS Collaboration, Charged-particle nuclear modification factors in PbPb and pPb collisions at $\sqrt{s_{NN}} = 5.02$ TeV, JHEP 04 (2017) 039.
[62] J. Adam, et al., ALICE Collaboration, Centrality dependence of the charged-particle multiplicity density at midrapidity in Pb-Pb Collisions at $\sqrt{s_{NN}} = 5.02$ TeV, Phys. Rev. Lett. 116 (2016) 222302.
[63] A.M. Sirunyan, et al., CMS Collaboration, Charged-particle nuclear modification factors in XeXe collisions at $\sqrt{s_{nn}} = 5.44$ TeV, JHEP 1810 (2018) 138.
[64] A. Adare, et al., PHENIX Collaboration, Transverse energy production and charged-particle multiplicity at midrapidity in various systems from $\sqrt{s_{NN}} =$ 7.7 to 200 GeV, Phys. Rev. C 93 (2016) 024901.
[65] J. Adam, et al., ALICE Collaboration, Measurement of transverse energy at midrapidity in Pb-Pb collisions at $\sqrt{s_{NN}} = 2.76$ TeV, Phys. Rev. C. 94 (2016) 034903.
[66] P.F. Kolb, U. Heinz, Hydrodynamic description of ultrarelativistic heavy-ion collisions Preprint, arXiv:nucl-th/0305084 [nucl-th].
[67] S. Borsanyi, et al., Calculation of the axion mass based on high-temperature lattice quantum chromodynamics, Nature 539 (7627) (2016) 69.
[68] S. Peigné, A. Peshier, Collisional energy loss of a fast heavy quark in a quark-gluon plasma, Phys. Rev. D 77 (2008) 114017.